

Glucose Directly Links to Lipid Metabolism through High Affinity Interaction with Peroxisome Proliferator-activated Receptor α *

Received for publication, June 21, 2007, and in revised form, November 28, 2007 Published, JBC Papers in Press, November 30, 2007, DOI 10.1074/jbc.M705138200

Heather A. Hostetler[‡], Huan Huang[‡], Ann B. Kier[§], and Friedhelm Schroeder^{‡,1}

From the Departments of [‡]Physiology and Pharmacology and [§]Pathobiology, Texas A&M University, College Station, Texas 77843-4467

The pathophysiology of diabetes is characterized not only by elevated glucose but also elevated long chain fatty acid levels. We show for the first time that the peroxisome proliferator-activated receptor- α (PPAR α) binds glucose and glucose metabolites with high affinity, resulting in significantly altered PPAR α secondary structure. Glucose decreased PPAR α interaction with fatty acid metabolites and steroid receptor coactivator-1 while increasing PPAR α interaction with DNA. Concomitantly, glucose increased PPAR α interaction with steroid receptor coactivator-1, DNA binding, and transactivation of β -oxidation pathways in the presence of activating ligands. Heterodimerization of PPAR α to the retinoid X receptor- α resulted in even larger increases in transactivation with the addition of glucose. These data suggest that PPAR α is responsible for maintaining energy homeostasis through a concentration-dependent regulation of both lipids and sugars and that hyperglycemic injury mediated by PPAR α occurs not only indirectly through elevated long chain fatty acid levels but also through direct action of glucose on PPAR α .

Energy homeostasis is a highly complex and strictly regulated process. Free fatty acids compete with glucose for oxidation, and increased free fatty acid concentrations are associated with reduced muscle glycogen synthesis. Dysregulation at any step may elicit severe pathophysiological complications, as seen in diabetes. Maintained low levels of blood glucose are critical for preventing or delaying the clinical complications of diabetes, such as insulin resistance and cardiovascular disease (1). Although the liver plays essential roles in the control of blood glucose levels by modulating gluconeogenesis and glycogen synthesis, the specific mechanism(s) of this regulation is unclear. Several studies suggest that peroxisome proliferator-activated receptor α (PPAR α),² a ligand-regulated transcrip-

tion factor belonging to the nuclear hormone receptor superfamily, contributes to this regulation.

PPAR α is highly expressed in liver and is the target of potent hypolipidemic drugs, such as fibrates, used to treat cardiovascular disease (2). Although a variety of compounds bind and activate PPAR α , long chain fatty acids (LCFA) and their metabolites (*i.e.* long chain fatty acyl-CoAs, LCFA-CoA) function as high affinity, endogenous ligands (3–5), which could play an important role because diabetes is characterized not only by elevated glucose levels but also elevated LCFA and LCFA-CoA levels (6). Ligand binding initiates PPAR α transcription of multiple genes in fatty acid and glucose metabolism while concomitantly down-regulating genes in insulin signaling (7–9). Furthermore, expression of PPAR α is elevated in humans with type 2 diabetes (10), and PPAR α -null mice are protected from high fat diet-induced insulin resistance (11).

EXPERIMENTAL PROCEDURES

Protein Expression and Purification—The bacterial expression vector containing murine PPAR α (pET-PPAR α Δ AB) was expressed in the BL21(DE3)pLysS strain of *Escherichia coli* as described (3) and purified by cation exchange and size exclusion chromatography. Dialyzation, quantification, and protein quality were analyzed as previously described (4). This truncated version, rather than the full-length protein, was used for the pure protein studies because of solubility issues with the full-length protein and difficulties with its recombinant purification. Although this recombinant protein was lacking the A/B domain, the entire DNA-binding domain and ligand-binding domain were present. This truncated version is expected to show ligand binding properties identical to those of the full-length receptor based upon similar experiments with PPAR γ (12, 13). However, the A/B region of PPAR α has been found to have a transactivating function through the ligand-independent transactivation domain (AF-1 activity) (14), and for this reason, the full-length protein was used for the coimmunoprecipitation, DNA binding, and transactivation assays.

Glucose Binding Assay—The direct binding of glucose and the glucose metabolites (glucose-1-phosphate, G-1-P; glucose-6-phosphate, G-6-P) to 100 nM PPAR α Δ AB was determined by quenching of intrinsic PPAR α Δ AB aromatic amino acid fluo-

* This work was supported in part by the United States Public Health Service National Institutes of Health Grant DK41402 (to F. S. and A. B. K.), Administrative Supplement "Drug Screening Program for Diabetic Complications" to Grant DK41402 (to F. S. and A. B. K.), National Institutes of Health National Research Service Award DK066732 (to H. A. H.), and National Institutes of Health K99 Award DK77573 (to H. A. H.). The costs of publication of this article were defrayed in part by the payment of page charges. This article must therefore be hereby marked "advertisement" in accordance with 18 U.S.C. Section 1734 solely to indicate this fact.

¹ To whom correspondence should be addressed: Dept. of Physiology and Pharmacology, Texas A & M University, TVMC, College Station, TX 77843-4466. Tel.: 979-862-1433; Fax: 979-862-4929; E-mail: fschroeder@cvm.tamu.edu.

² The abbreviations used are: PPAR α , peroxisome proliferator-activated receptor α ; LCFA, long chain fatty acid; SRC-1, steroid receptor coactivator-1; RXR α , retinoid X receptor α ; G-1-P, glucose-1-phosphate; G-6-P, glucose-6-phosphate; PPRe, peroxisome proliferator response element; L-FABP, liver fatty acid-binding protein; DMEM, Dulbecco's modified Eagle's medium; PBS, phosphate-buffered saline; LSCM, laser scanning confocal microscopy.

rescence as previously described for nonfluorescent fatty acids and fatty acyl-CoAs (4, 5). Emission spectra from 300 to 400 nm were obtained at 24 °C by excitation at 280 nm with a PC1 photon counting spectrofluorometer (ISS Inc., Champaign, IL). The data were corrected for background (buffer, fluorescent ligands, and solvent effects), and the maximal intensities were used to calculate the dissociation constant (K_d) and the number of binding sites as previously described (4).

Autoglycation—To determine whether PPAR α autoglycation could occur under the conditions of the binding and circular dichroism assays, 100 nM PPAR α Δ AB was incubated with 1 μ M 2-deoxy-d-[1-³H]glucose supplemented with cold glucose for a final concentration of 20 mM at room temperature for 30 min in PBS. Following incubation, the mixture was applied to a filtration device (Microcon; Millipore, Bedford, MA) and centrifuged to remove free glucose. The resulting protein-glucose mixture was washed three times with excess glucose to determine whether the radioactive glucose was permanently bound (covalent) or could be removed. Each flow-through and retentate was examined for activity with a scintillation counter as compared with no protein controls.

Circular Dichroism—Circular dichroic spectra of 0.8 μ M PPAR α Δ AB were taken in the absence and presence of glucose and glucose metabolites with a J-710 spectropolarimeter (JASCO Inc., Easton, MD) as previously described (4, 5). Glucose concentrations below (0.6 μ M) and above (6 μ M) a 1:1 protein to glucose ratio were examined, whereas the physiological concentrations found in the unstressed rat liver (11 μ M G-1-P, 0.2 mM G-6-P) were examined for metabolites (15). Ten scans were averaged for the percentage of composition of secondary structures by three different methods (SELCON3, CDSSTR, and CONTIN/LL) with the software package CDPro (16) as previously described (4).

Fluorescent Fatty Acid and Acyl-CoA Binding—PPAR α binding affinity for a fluorescent 16 carbon fatty acid analog (BODIPY C-16, Molecular Probes, Eugene, OR) and its CoA thioester (BODIPY C-16-CoA, produced and purified as previously described for acyl-CoAs (4)) was determined. Because of solubility issues with the BODIPY compounds, PPAR α Δ AB binding affinity was first determined by quenching of intrinsic PPAR α Δ AB aromatic amino acid fluorescence as described above for glucose. Because both glucose and the BODIPY compounds resulted in quenching of PPAR α Δ AB intrinsic fluorescence, BODIPY fluorescence was used for determining the effect of glucose on BODIPY fatty acid and fatty acyl-CoA binding. For binding assays, 100 nM PPAR α Δ AB protein was titrated with increasing concentrations of BODIPY C-16 or BODIPY C-16-CoA in the presence of 6 mM glucose. For displacement assays, binding of 100 nM PPAR α Δ AB protein with 50 nM BODIPY C-16 or BODIPY C-16-CoA was measured, and the effect of glucose on BODIPY displacement was measured as a decrease in fluorescence intensity. Emission spectra from 490 to 540 nm were obtained at 24 °C by excitation at 460 nm with a PC1 photon counting spectrofluorometer (ISS Inc., Champaign, IL). The data were corrected for background (buffer, fluorescent ligands, and solvent effects), and the maximal intensities were used to calculate the percentage of change in BODIPY C-16 and BODIPY C-16-CoA binding as well as the dissocia-

tion constant (K_d), inhibition constant (K_i), and number of binding sites as previously described (4).

Cell Culture—COS-7 cells (ATCC, Manassas, VA) were grown in DMEM (Invitrogen) supplemented with 10% fetal bovine serum (Invitrogen) at 37 °C with 5% CO₂ in a humidified chamber. Murine L-cell (L arpt⁻ tk⁻) fibroblasts were grown as previously described (17).

Coimmunoprecipitation Assays—COS-7 cells were transfected with mammalian expression vectors for full-length PPAR α (pSG5-PPAR α) (18) and SRC-1 (pcDNA3 Δ -SRC-1-Myc) (19) with Lipofectamine 2000 reagent (Invitrogen) according to the manufacturer's instructions. The medium was replaced with serum-free, glucose-free DMEM (Invitrogen) 20 h post-transfection and incubated for an additional 2 h. Cell lysis, coimmunoprecipitation, and Western blot procedures were conducted as previously described for liver homogenate with fatty acyl-CoAs (5). Briefly, 2 mg of cell lysate was mixed with activating ligand and/or glucose as indicated in the figure legend, and the cell lysates were incubated with antibody-linked resin for 1.5 h at room temperature. Eluted proteins were examined by Western blot analysis. The values were normalized to the amount of PPAR α protein detected, and the samples in the presence of 10 μ M clofibric acid and in the absence of glucose were arbitrarily set to 100%.

NoShift DNA Binding Assays—Full-length PPAR α and RXR α RNA was prepared from the mammalian expression plasmids pSG5-PPAR α (18) and pSG5-mRXR α (20) and translated with the TNT[®]-coupled reticulocyte lysate system as recommended by the manufacturer (Promega Corp., Madison, WI). To obtain quantitative data, the NoShift[™]II PPAR transcription factor assay kit (Novagen, Madison, WI) was utilized per the manufacturer's instructions with *in vitro* synthesized full-length PPAR α (2 μ l) and RXR α (2 μ l) lysates. Glucose was added to the incubation mixtures as indicated in the figure legend. Luminescence was measured with a Microlite ML3000 microtiter plate luminometer (Dynatech Laboratories, Inc., Chantilly, VA). The values are presented as the percentage of binding where clofibric acid-induced DNA binding (positive control) is arbitrarily set to 100%.

Transactivation Assays—COS-7 cells grown in 6-well culture plates were transfected with 1 μ g of each full-length mammalian expression vector (pSG5-PPAR α (18) and pSG5-mRXR α (20)) or empty plasmid (pSG5; Stratagene, La Jolla, CA), 1 μ g of the reporter construct PPRE₃-TK-LUC (21), and 0.05 μ g of the internal transfection control plasmid pRL-CMV (Promega Corp., Madison, WI). Transfections were performed with Lipofectamine 2000 reagent (Invitrogen) according to the manufacturer's instructions. Following transfection incubation, the medium was replaced with serum-free, glucose-free DMEM (Invitrogen) for 2 h, and then the ligands were added, and the cells were grown for an additional 24 h. Arachidonic acid was added to cells as a complex with bovine serum albumin as previously described (22). To ensure adequate nuclear levels of these ligands (clofibric acid, arachidonic acid, and glucose) for interaction with PPAR α (21, 23, 24), higher concentrations were used for the cell-based transactivation experiments than for the pure protein experiments. Firefly luciferase activity, normalized to *Renilla* luciferase (for transfection efficiency), was

determined with the dual luciferase reporter assay system (Promega, Madison, WI) according to the manufacturer's instructions. Luminescence was measured with a Microlite ML3000 microtiter plate luminometer (Dynatech Laboratories, Inc.).

Determination of Intracellular Glucose Concentration and Nuclear Distribution—COS-7 and L-cells were seeded onto 10-cm culture dishes (for determination of total intracellular glucose concentration) or Lab-Tek chambered cover glass (for determination of nuclear distribution) and cultured as described above for 24 h. The cells were washed two times with PBS and incubated at 37 °C for 3 h in serum-free, glucose-free DMEM (Invitrogen) to ensure utilization of exogenous glucose.

For total intracellular glucose determination and nuclei isolations, the media were replaced with fresh serum-free, glucose-free DMEM supplemented with either 6 μ M or 6 mM glucose, and the cells were incubated for an additional 30 min or 2 h at 37 °C. Following incubation, the culture media were removed and examined for glucose content as compared with controls. The cells were washed twice with cold PBS and placed on ice. For total intracellular glucose concentration, the cells were lysed in M-PER[®] buffer (Pierce) containing 150 mM sodium chloride and protease inhibitors for 10 min at room temperature. Protein content of cell lysate was determined by BCA protein assay (Pierce) and used to estimate total cell number. The nuclei were isolated with the Nuclei EZ Prep nuclei isolation Kit (Sigma) per the manufacturer's instructions. The nuclei were diluted and counted with a hemocytometer according to the manufacturer's instructions (Sigma). Glucose content for cell lysates, nuclei, and cytoplasmic components was determined by the Autokit Glucose CII (Wako Chemicals USA, Richmond, VA) per the manufacturer's instructions.

For determination of glucose distribution, the medium was replaced with PBS containing 1.25 μ M Syto59 DNA-binding dye (Molecular Probes, Eugene, OR) and incubated at room temperature for 30 min, and background images were taken. The cells were washed with PBS and incubated at 37 °C for 20 min with PBS containing 6 μ M 6-NBD-glucose, a fluorescent, nonhydrolyzable glucose analog (Molecular Probes, Eugene, OR). Following incubation, the cells were washed with PBS and imaged in fresh PBS (see below).

Laser Scanning Confocal Microscopy (LSCM)—LSCM studies were performed with a $\times 63$ Plan-Fluor oil immersion objective, N.A.1.45, an Axiovert 135 microscope (Zeiss, Carl Zeiss Inc., Thornwood, NY), and MRC-1024 fluorescence imaging system (Bio-Rad) as previously described (17). The Syto59 and NBD-glucose probes were excited with laser 488/568 lines with a krypton-argon laser (Coherent, Sunnyvale, CA). Emission from NBD-glucose was recorded by a photomultiplier after passing through a 522/D35 emission filter and emission from Syto59 was collected with a 680/32 emission filter, both under manual gain and black level control. The objective was focused to acquire 0.3- μ m confocal slice images through median sections of cells in the field. The cells were excited for 0.1-s intervals, regulated by a computer-controlled shutter and Laser Sharp software (Bio-Rad). The images were analyzed using Image J software from the National Institutes of Health (rsb.info.nih.gov/ij/). The number of pixels of NBD-glucose colocalized with the Syto59 (nuclear localization) as well as the

number of NBD-glucose pixels not colocalized with Syto59 (cytoplasmic) were averaged over several replicates ($n = 5$, ~ 20 cells each) to obtain the percentage of distribution of NBD-glucose.

Calculation of Intracellular and Nuclear Glucose Concentrations—The amount of NBD-glucose in the nucleus was calculated based upon the percentage of distribution (determined by LSCM fluorescence imaging) in nuclei *versus* cytoplasm (plus plasma membrane) from the medial cross-sectional plane. Estimated cellular protein concentration and cellular volumes were as described (25), and final concentrations were calculated from the amount of glucose in the whole cell or nucleus divided by the estimated respective volumes of the whole cell and nucleus. To determine whether NBD-glucose distribution was similar to glucose distribution, the amount of glucose in purified nuclei was compared with the amount of glucose in the cytoplasmic fraction.

Calculation of Nuclear PPAR α Concentrations—Liver homogenates from male C57BL/6 mice were prepared and quantified as previously described for coimmunoprecipitation (4). Liver homogenates and known amounts of purified PPAR α protein (Novus Biologicals, Littleton, CO) were separated by SDS-PAGE and transferred to nitrocellulose membrane, and Western blot analysis was performed as described previously for PPAR α coimmunoprecipitation (4). Protein bands were quantified by densitometry, utilizing a single-chip charge-coupled device video camera FluorChemimager and accompanying FluorChem image analysis software from Alpha Innotech (San Leandro, CA). Total cell number, intracellular volume, and nuclear volume were 1.7×10^8 cells/g of liver, 6.2 pL, and 1.8 pL, respectively, as determined previously (26, 27). Final concentrations were calculated from the amount of PPAR α protein in the whole cell or nucleus divided by the estimated respective volumes of the whole cell and nucleus.

Statistical Analysis—All of the results are expressed as the means \pm S.E. Statistical significance between samples in the presence or absence of glucose was determined by using the Student's *t* test with $p < 0.05$.

RESULTS

PPAR α Exhibits High Affinity for Glucose and Glucose Metabolites—To determine whether glucose itself directly affects PPAR α , PPAR α binding of glucose and glucose metabolites was examined. The addition of glucose decreased the intrinsic fluorescence of PPAR α , corresponding to ligand binding (4). This change in fluorescence with increasing glucose yielded a sharp saturation curve with a maximal change noted at ~ 100 nM (Fig. 1A), which transformed into a linear reciprocal plot (*inset*), indicating high affinity of PPAR α for glucose at a single binding site. Multiple replicates ($n = 4$) yielded a $K_d = 2.0 \pm 0.4$ nM, similar to those obtained previously for unsaturated LCFA and LCFA-CoA (3–5). This is a ligand binding effect, not a covalent modification, because bound radiolabeled glucose was displaced with an excess of nonradiolabeled glucose under the conditions utilized in these assays (data not shown). This suggests that PPAR α is highly sensitive to glucose prior to any physical manifestation, such as autoglycation, seen much later in chronic instances such as diabetes. To determine

specificity for glucose, PPAR α affinity for glucose-1-phosphate (G-1-P; Fig. 1B) and glucose-6-phosphate (G-6-P; Fig. 1C) was examined. Both glucose metabolites decreased PPAR α fluorescence, indicating strong saturable binding at a single site; G-1-P $K_d = 25.3 \pm 3.5$ nM, G-6-P $K_d = 63.2 \pm 6.6$ nM. These data demonstrate that both glucose and its metabolites directly interact with PPAR α with high affinity.

PPAR α Binding to Glucose Results in Changes to PPAR α Secondary Structure—To determine whether ligand binding altered PPAR α conformation, CD was used to determine glucose effects on PPAR α secondary structure. The CD spectra of PPAR α exhibited a large peak in molar ellipticity at 192 nm and two concomitant negative peaks at 207 and 222 nm (Fig. 1D and E, filled circles). Because maximal glucose binding was noted near a 1:1 glucose to PPAR α protein molar ratio, lower (3:4, 0.6 μ M, open circles) and higher (15:2, 6 μ M, open triangles) ratios than 1:1 were examined, both resulting in diminished minima and maxima (Fig. 1D). Although glucose metabolites (Fig. 1E; G-1-P, open circles; G-6-P, open triangles) significantly altered PPAR α spectra in a similar manner as glucose, higher concentrations were required to elicit maximal CD changes, consistent with their weaker affinity. When multiple replicates ($n = 3-4$) of CD spectra were analyzed for the percentage of composition of α -helices, β -sheets, turns, and unordered structures, the

addition of 0.6 and 6 μ M glucose, 11 μ M G-1-P, and 0.2 mM G-6-P resulted in similar changes (Table 1). Glucose and the examined metabolites elicited an overall decrease in α -helices, an increase in β -sheets, and increases in turns and unordered structures, similar to the effects of LCFA-CoA binding (4).

Glucose Interferes with PPAR α Binding to Fatty Acyl-CoA—Because glucose binding resulted in similar affinities and structural changes as previously reported for LCFA and LCFA-CoA binding, the ability of glucose to alter PPAR α interaction with lipidic ligands was examined. PPAR α binding of BODIPY-C16, a fluorescent 16 carbon fatty acid analog, was strongly saturable at a single binding site (Fig. 2C, circles). Binding of the acyl-CoA derivative (BODIPY C-16-CoA) was also strongly saturable at a single binding site (Fig. 2D, circles). Multiple replicates ($n = 4$) yielded K_d values of 7.1 ± 1.3 and 17.6 ± 2.4 nM for BODIPY-C16 and BODIPY C-16-CoA, respectively, indicating high binding affinity.

The ability of glucose and glucose metabolites to displace these fluorescent lipids from the PPAR α -binding pocket was then examined. Although the addition of glucose, G-1-P, G-6-P, or phosphate (negative control) had only minor effects on BODIPY C-16 fatty acid binding (Fig. 2A, filled bars), significant differences were noted for BODIPY C-16-CoA (Fig. 2A, open bars). The addition of 0.6 and 6 mM glucose resulted in significant decreases in acyl-CoA binding, and both G-1-P and G-6-P also significantly decreased acyl-CoA binding but to a lesser extent. Although acyl-CoA displacement leveled off ($\sim 35\%$) by 60 μ M glucose, even concentrations as low as 60 nM resulted in significant decreases (Fig. 2B). The binding affinity of glucose was found to be slightly lower ($K_i = 13.3 \pm 1.2$ nM) by displacement than that obtained by direct binding. To determine whether glucose changed the binding affinity or simply displaced these lipidic ligands, lipid binding assays were repeated in the presence of excess glucose. Although the shape of the binding curve for BODIPY C-16 in the presence of glucose (Fig. 2C, triangles) differed slightly from that without glucose, the binding affinity was similar ($K_d = 5.0 \pm 0.7$

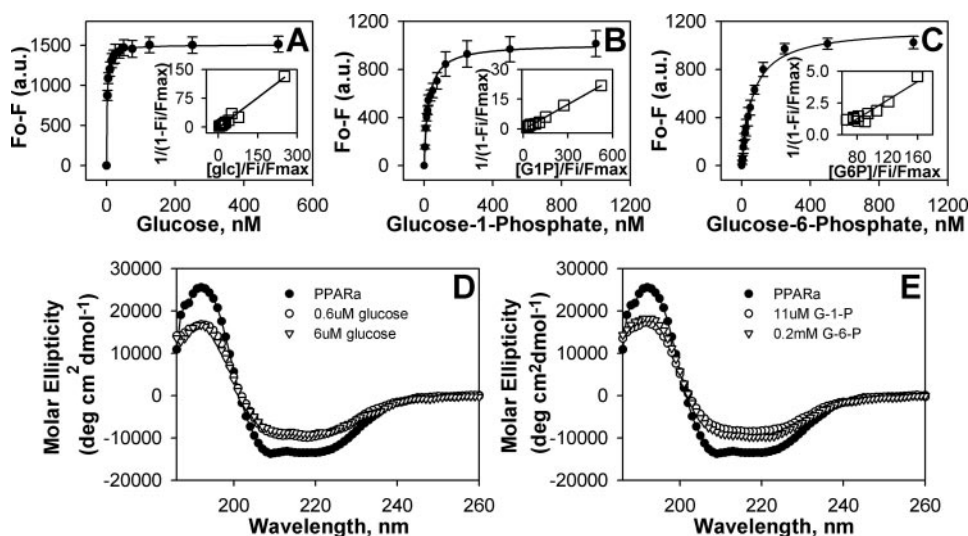


FIGURE 1. PPAR α binds glucose and glucose metabolites with high affinity, resulting in conformational changes. Binding curve of the change in PPAR α intrinsic fluorescence upon titration with glucose (A), glucose-1-phosphate (B), and glucose-6-phosphate (C). The values are presented as the mean value ($n = 4$) \pm the standard error. The insets are double reciprocal plots of the mean binding curve data presented in each panel. A representative circular dichroic spectra ($n = 3-4$, 10 scans each) of PPAR α (D and E, filled circles) in the presence of 0.6 μ M glucose (D, open circles); 6 μ M glucose (D, open triangles); 11 μ M G-1-P (E, open circles); and 0.2 mM G-6-P (E, open triangles).

TABLE 1

Percentage of composition of PPAR α secondary structures in the presence of glucose metabolites

The values represent the mean percentages of composition \pm the standard error ($n = 3-4$). Significant differences were determined by Student's t test.

	α -Helices		β -Sheets		Turns	Unordered
	Regular	Distorted	Regular	Distorted		
	%	%	%	%	%	%
PPAR α	23.34 \pm 0.28	15.60 \pm 0.08	8.29 \pm 0.12	6.82 \pm 0.08	19.13 \pm 0.21	26.86 \pm 0.17
0.6 μ M glucose	15.23 \pm 0.47 ^a	12.09 \pm 0.22 ^a	13.14 \pm 0.87 ^a	8.43 \pm 0.29 ^a	21.61 \pm 0.53 ^a	29.11 \pm 0.56 ^a
6 μ M glucose	15.71 \pm 0.22 ^a	12.57 \pm 0.13 ^a	12.77 \pm 0.65 ^a	8.58 \pm 0.22 ^a	21.53 \pm 0.41 ^a	28.00 \pm 0.50 ^a
11 μ M G-1-P	13.47 \pm 0.35 ^a	11.40 \pm 0.31 ^a	14.53 \pm 0.91 ^a	8.71 \pm 0.30 ^a	21.66 \pm 0.44 ^a	29.96 \pm 0.58 ^a
0.2 mM G-6-P	17.21 \pm 0.38 ^a	12.83 \pm 0.16 ^a	12.08 \pm 0.81 ^a	8.14 \pm 0.23 ^a	21.34 \pm 0.61 ^a	28.87 \pm 0.87 ^a

^a $p < 0.01$.

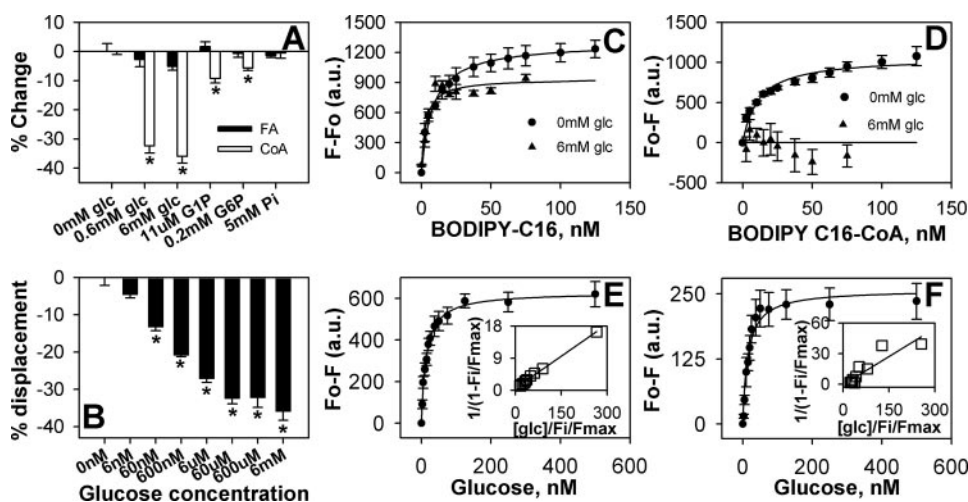


FIGURE 2. Glucose binding inhibits fatty acid metabolite binding but lipid binding does not inhibit glucose binding. The percentage of change in PPAR α binding to BODIPY C-16 fatty acid (filled bars) and BODIPY C-16-CoA (open bars) in the presence of glucose and glucose metabolites (A). Examination of the effect of lower concentrations of glucose on PPAR α binding to BODIPY C-16-CoA (B) shows that this effect is saturable, allowing for calculation of glucose affinity by BODIPY C-16-CoA displacement as described under "Experimental Procedures." Binding of PPAR α to BODIPY C-16 fatty acid (C) is similar in the absence (circles) and presence of 6 mM glucose (triangles), both resulting in high affinity binding. Binding of PPAR α to BODIPY C-16-CoA (D) in the absence (circles) of glucose results in strong binding, whereas the presence of 6 mM glucose (triangles) results in no BODIPY C-16 CoA binding. Glucose binding in the presence of 10 μ M BODIPY C-16 fatty acid (E) and BODIPY C-16-CoA (F) still shows strong saturable binding. The values are the mean values ($n = 4-5$) \pm the standard error. Insets, double reciprocal plots of the mean binding curve data. Asterisks represent significant deviation from no glucose controls ($p < 0.05$).

nM). In contrast, no BODIPY C-16-CoA binding was noted in the presence of glucose (Fig. 2D, triangles). Although the presence of excess BODIPY C-16 fatty acid (Fig. 2E) or acyl-CoA (Fig. 2F) did not prevent glucose binding, a 6–7-fold decrease in glucose affinity was noted (K_d values of 13.8 ± 1.8 and 14.6 ± 3.4 nM, respectively). This is similar to the affinity obtained for glucose through the displacement of BODIPY C-16-CoA.

Glucose Decreases Coactivator Recruitment of PPAR α under Basal Conditions while Increasing Coactivator Recruitment of PPAR α in the Presence of Activating Lipidic Ligands—In homogenates from COS-7 cells grown in serum-free, glucose-free medium, the addition of glucose decreased PPAR α interaction with the steroid receptor coactivator-1 (SRC-1) in a concentration-dependent manner (Fig. 3A). Although larger concentrations of glucose inhibited PPAR α interaction with SRC-1 more than weaker concentrations, even 0.6 μ M glucose resulted in a significant decrease in SRC-1 recruitment, suggesting that glucose inhibits PPAR α regulated transcription in the absence of other ligands. In contrast, in homogenates from COS-7 cells incubated with arachidonic acid (Fig. 3B) or clofibrate (Fig. 3C), low levels of glucose (6 μ M) significantly increased PPAR α interaction with SRC-1, whereas higher concentrations of glucose (above 60 μ M) did not alter SRC-1 recruitment. This suggests that PPAR α may regulate both lipid and sugar metabolism through a ligand concentration-dependent selection.

Glucose Increases PPAR α -RXR α Binding to DNA—Because PPAR α heterodimerization to RXR α increases DNA binding (21), *in vitro* synthesized PPAR α and RXR α protein was used to determine the effect of glucose on DNA binding. To quantitate this effect of DNA binding, a NoShift assay was utilized. Under basal conditions, the addition of glucose (6 nM to 6 mM) resulted in more DNA binding by PPAR α -RXR α than seen in the

absence of glucose (Fig. 3D). This effect of DNA binding increased with increasing glucose concentrations, with the effect plateauing around 6 μ M. In the presence of arachidonic acid, the addition of glucose increased DNA binding until 0.6 μ M, at which point DNA binding plateaued (Fig. 3E). In the presence of clofibrate, the addition of glucose increased DNA binding until about 60 nM (Fig. 3F). In each case, the addition of glucose significantly increased PPAR α -RXR α heterodimer binding to the PPRE.

Glucose Increases Transactivation of PPAR α -RXR α Heterodimers—Because PPAR α forms heterodimers with RXR α to induce transactivation (21, 23), the cells were cotransfected with PPAR α alone, RXR α alone, PPAR α and RXR α , or pSG5 empty vector. PPAR α transactivation was measured as response of firefly luciferase upon interaction of

PPAR α with the PPRE of the acyl-CoA oxidase promoter (21) normalized to *Renilla* luciferase. Although only slight changes in transactivation of the acyl-CoA oxidase luciferase fusion protein were noted for the addition of glucose to PPAR α in the absence of RXR α or added lipidic ligands, concentrations between 0.6 and 2.4 mM resulted in decreased activation, whereas 6 mM glucose had no effect (Fig. 3G). Similar results were obtained in the presence of 10 μ M arachidonic acid (Fig. 3H). However, the addition of 10 μ M clofibrate resulted in approximately a 3-fold increase in activation but only at 6 mM glucose (Fig. 3I). Glucose had no significant effect on RXR α transactivation (Fig. 3, G–I).

In the presence or absence of clofibrate, transcriptional activity of PPAR α was increased ~ 3.7 -fold by the presence of RXR α (Fig. 3, G and I, open bars), whereas in the presence of arachidonic acid, transcription only increased 2.5-fold (Fig. 3H, open bars). The addition of glucose increased transcriptional activity of PPAR α -RXR α heterodimers in both the presence and absence of ligands. In the absence of ligand, PPAR α -RXR α activity increased with increasing glucose concentration from 0.6 to 2.4 mM, whereas activity levels were only slightly higher with 6 mM glucose than in the absence of glucose (Fig. 3G). Arachidonic acid-induced activity was increased 1.4-fold with the addition of 2.4 mM glucose and almost 3-fold with 6 mM glucose (Fig. 3H). Clofibrate-induced activity increased with increasing glucose concentration, with 6 mM glucose resulting in a 2.5-fold increase (Fig. 3I). Although arachidonic acid-induced expression resulted in the largest change compared with no glucose controls, clofibrate-induced expression in the presence of 6 mM glucose resulted in the highest amount of expression.

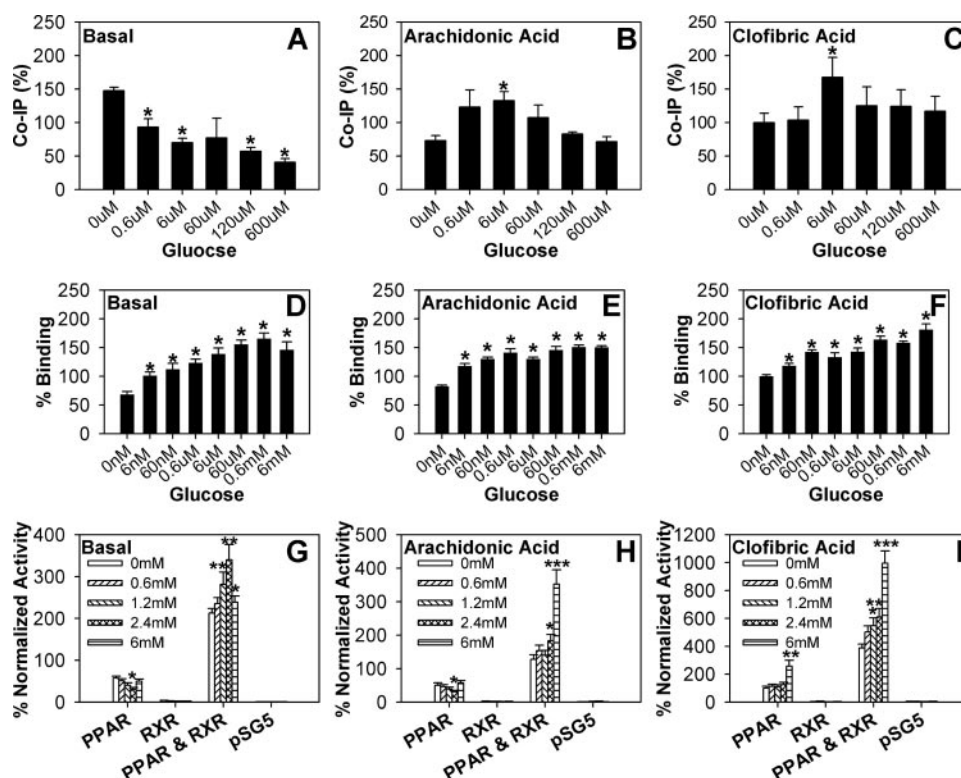


FIGURE 3. Glucose alters PPAR α interaction with coactivators, DNA binding, and transactivation. COS-7 cells were transfected with mammalian expression vectors for PPAR α and SRC-1 as described under "Experimental Procedures." Glucose was added to cell lysates, and the effect of glucose on coimmunoprecipitation of SRC-1 with PPAR α in the absence (A) or presence of activating ligands (arachidonic acid, B; clofibric acid, C). The values were normalized to the amount of PPAR α protein detected, and the samples in the presence of 10 μ M clofibric acid and in the absence of glucose were arbitrarily set to 100%. The effect of glucose on PPAR α -RXR α heterodimer DNA binding with a quantitative NoShiftIt assay (Novagen) under basal (D), arachidonic acid-induced (E), and clofibric acid-induced (F) conditions. The values are presented as percentages of binding where clofibric acid-induced DNA binding (positive control) is arbitrarily set to 100%. COS-7 cells transfected with PPAR α , RXR α , PPAR α , and RXR α , or control pSG5 empty vector were analyzed for basal (G), 10 μ M arachidonic acid-induced (H), and 10 μ M clofibric acid-induced (I) transactivation of an acyl-CoA oxidase reporter construct in the presence of 0 mM glucose (open bars), 0.6 mM glucose (diagonally upward bars), 1.2 mM glucose (diagonally downward bars), 2.4 mM glucose (hatched bars), and 6 mM glucose (horizontally lined bars). The transactivation values are presented as percentages of firefly luciferase activity normalized to *Renilla* luciferase (internal control) where clofibric acid-induced PPAR α activity in the absence of glucose (positive control) is arbitrarily set to 100%. The bar graph values represent the mean values ($n = 3$) \pm the standard error. Asterisks represent significant differences for the addition of glucose ($p < 0.05$).

Nuclear Glucose Concentration Is in the Low Micromolar Range while PPAR α Concentration Is \sim 10-fold Higher—Because of the inability to remove all serum from liver tissues by a noninvasive technique (*i.e.* without disrupting the cellular glucose equilibrium) and because serum glucose levels are in the millimolar range (15), cultured cells were used as a model to estimate total intracellular and nuclear glucose levels in the presence of 6 μ M and 6 mM extracellular glucose. Intracellular glucose was determined by a chemical assay, whereas nuclear distribution was determined by a noninvasive LSCM technique, as described under "Experimental Procedures." LSCM of NBD-glucose showed that \sim 11.3% of the intracellular NBD-glucose was nuclear in COS-7 cells (Fig. 4, A and C), whereas only 5.9% NBD-glucose was nuclear in L-cells (Fig. 4, B and D). A similar distribution was obtained when nuclei and cytoplasmic fractions were examined by chemical assay under the same conditions (*i.e.* 6 μ M glucose and 30 min incubation), although some variation was noted between 30-min and 2-h incubations (Table 2). The estimated intracellular glucose concentrations

ranged from 25 to 47 μ M, whereas nuclear concentrations ranged from 6 to 22 μ M, depending upon the cell line and the length of incubation (Table 3). By Western blot analysis (Fig. 4E), PPAR α constitutes \sim 1.6 \pm 0.2% of total liver proteins. Because the majority of PPAR α protein is nuclear in cultured L-cell fibroblasts (25) and cultured mouse primary hepatocytes (28),³ the estimated nuclear concentration of PPAR α was 309 \pm 28 μ M.

DISCUSSION

Although several studies have suggested that PPAR α may function to regulate glucose homeostasis, it was believed that such regulation occurred only as an indirect action of fatty acid on PPAR α . Because hallmarks of ligand-activated nuclear receptors are high ligand affinity, ligand-induced conformational change, and ligand-induced alteration in receptor activity, the experiments herein demonstrate for the first time that glucose itself is an endogenous ligand of PPAR α . Furthermore, glucose was able to alter the effects of other endogenous PPAR α ligands by inhibiting LCFA-CoA binding while enhancing the transcriptional effects of fatty acids.

Because the first step of β -oxidation is the conversion of LCFA to LCFA-CoA, it may seem counterintuitive that the presence of glucose decreased the affinity of PPAR α for fatty acyl-CoA ligands while increasing PPAR α activation of a β -oxidation enzyme. However, it should be noted that not only LCFA-CoAs but also unsaturated LCFA are PPAR α activators (3–5, 29–31), and LCFA binding to PPAR α was unaltered by the presence of glucose. Further, in the absence of RXR α , the addition of glucose to PPAR α (with or without added arachidonic acid) resulted in decreased activation of the β -oxidation enzyme. Only in the presence of clofibric acid, a very potent PPAR α agonist, was an increase in activation seen. Earlier experiments (32, 33) have suggested that although LCFA binding induces PPAR α activation (agonists), a nonhydrolyzable LCFA-CoA represses PPAR α activity (antagonists). Thus, it is possible that glucose binding may function as a rheostat-like control mechanism to regulate LCFA or LCFA-CoA binding to PPAR α .

Sequence comparisons of the binding sites of several glucose-binding proteins suggest that three amino acids (aspara-

³ A. L. McIntosh, B. P. Atshaves, H. Huang, H. R. Payne, H. A. Hostetler, J. Davis, A. B. Kier, and F. Schroeder, unpublished observation.

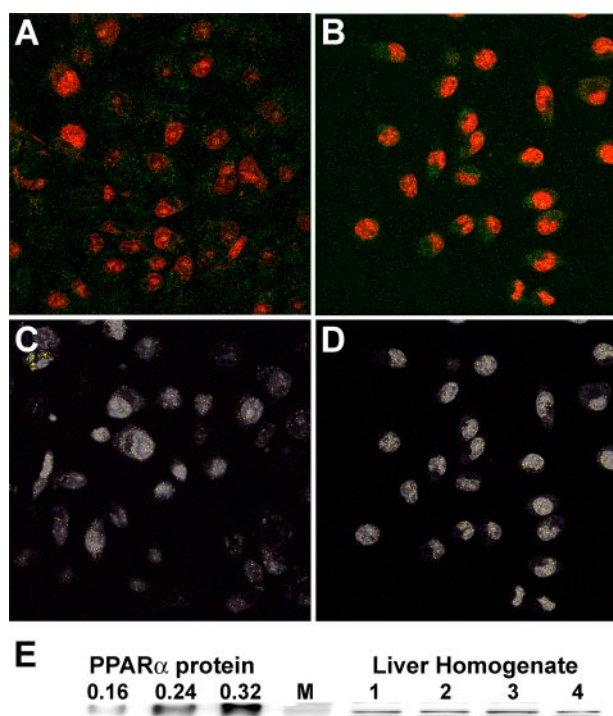


FIGURE 4. Nuclear glucose concentration was determined by NBD-glucose localization in cultured fibroblasts. A representative image ($n = 5$) for each cell line is presented. COS-7 (A and C) and L-cells (B and D) were incubated for 30 min with NBD-glucose (green pixels), stained with the nuclear dye SYTO59 (red pixels), and imaged by LSM as described under "Experimental Procedures." Colocalized pixels (C and D, yellow pixels) were measured and represent nuclear NBD-glucose. NBD-glucose not colocalizing with SYTO59 was measured as cytoplasmic. E, Western blot of 10 μ g samples of total protein from mouse liver homogenates ($n = 4$) as compared with known concentrations (0.16, 0.24, and 0.32 μ g) of purified recombinant PPAR α protein as a control to determine the relative amount of PPAR α in liver cells. Protein molecular mass marker (lane M) band approximately equals 50 kDa.

TABLE 2

Percentage of distribution of glucose in cultured cells by chemical analysis of purified nuclei and cytoplasmic fractions

The values represent the mean percentages of glucose ($n = 4 - 6$) in each fraction \pm the standard error.

	Glucose concentration for incubation	30 min of incubation		2 h of incubation	
		Cytoplasmic	Nuclear	Cytoplasmic	Nuclear
		%			
COS-7 cells	6 μ M	88.7 \pm 1.3	11.3 \pm 1.3	95.5 \pm 0.2	4.5 \pm 0.2
	6 mM	93.5 \pm 1.2	6.5 \pm 1.2	95.9 \pm 0.9	4.1 \pm 0.9
L-cells	6 μ M	94.5 \pm 0.6	5.5 \pm 0.6	95.3 \pm 0.8	4.7 \pm 0.8
	6 mM	93.2 \pm 4.5	6.8 \pm 4.5	92.6 \pm 2.1	7.4 \pm 2.1

TABLE 3

Estimated intracellular and nuclear glucose concentrations in cultured cells

The values represent the mean glucose concentrations ($n = 4$) \pm the standard error.

	Glucose concentration for incubation	Intracellular glucose concentration		Nuclear glucose concentration	
		30 min of incubation	2 h of incubation	30 min of incubation	2 h of incubation
		μ M			
COS-7 cells	6 μ M	36.56 \pm 1.89	31.91 \pm 1.08	17.95 \pm 0.93	15.66 \pm 0.53
11.3%	6 mM	41.40 \pm 4.19	45.49 \pm 1.88	20.32 \pm 2.06	22.33 \pm 0.92
L-cells	6 μ M	47.43 \pm 5.88	24.71 \pm 2.85	12.08 \pm 1.50	6.30 \pm 0.73
5.9%	6 mM	35.36 \pm 1.22	29.87 \pm 7.34	9.01 \pm 0.18	7.61 \pm 1.87

gine, aspartic acid, and glutamic acid) are essential for glucose binding (34). The PPAR α crystal structure (35) contains numerous asparagine, aspartic acid, and glutamic acid residues within the ligand-binding domain. If glucose and the CoA moiety of fatty acyl-CoA both bind to these residues, then glucose could prevent the fatty acyl-CoA from fitting into the PPAR α -binding pocket, while not disturbing fatty acid binding. Because the presence of glucose reduces acyl-CoA binding affinity, only the fatty acid would still be capable of binding to PPAR α to affect downstream regulation at elevated glucose concentrations. This has two important potential consequences: (i) because saturated fatty acids do not directly bind or activate PPAR α (3-5), the response to dietary fat (saturated *versus* unsaturated) may be altered and (ii) high levels of glucose and fatty acid may result in hyperactivation of PPAR α (36).

Although the exact concentrations of glucose, glucose metabolites, and PPAR α protein in cells expressing PPAR α is unknown and likely varies with diet, we have attempted to estimate these values to better relate the recombinant PPAR α protein ligand affinity to the more physiological experiments. The total amount of nuclear glucose was estimated to be in the micromolar range, similar to the glucose concentration noted for maximal changes in coactivator recruitment of PPAR α in the presence of arachidonic acid and clofibrate, and well within the range of glucose concentrations responsible for altering DNA binding. However, the proportion of the nuclear glucose available for interaction with PPAR α remains unknown. Because other proteins besides PPAR α can bind to glucose, it is possible that free nuclear glucose levels are substantially lower. For example, the liver fatty acid binding protein (L-FABP) is known to interact with glucose (15), and liver cell concentrations of L-FABP are high, in the range of 200-400 μ M, whereas nuclear concentrations of L-FABP are estimated to be \sim 43 μ M (17, 25). This suggests the existence of dynamic interrelationships between glucose, lipidic ligands (LCFA, LCFA-CoA, fibrates, etc.), and binding proteins in the nucleus (PPAR α , L-FABP, etc.).

Although the glucose concentrations utilized for the cell-based and cell lysate-based assays are higher than those used for the pure PPAR α based assays, it should be noted that this is the applied glucose concentration and does not necessarily represent the concentration of glucose available to interact with PPAR α . Intracellular glucose concentration is a function not only of glucose supply (*i.e.* extracellular glucose concentration) but also of the rate of glucose transport across the plasma membrane and the rate of glucose metabolism (37, 38). Because the rate of glucose transport into the cell is limited by the isoform type, number, and affinity of glucose transporters present at the cell surface (38), the intracellular glucose concentration is expected to vary between cell types and might be lower for cultured cells than for liver tissue. Moreover, the presence of hexokinases within the cells would rapidly convert free glucose into glucose-6-phosphate, again altering the intracellular or nuclear glucose levels available for interaction with PPAR α . Consequently, not only for cell-based assays but also for cell lysate-based assays, additional factors may contribute to the higher glucose concentration needed to elicit significant effects as compared with *in vitro* pure PPAR α based assays. This would

include: (i) endogenous glucose; (ii) glucose metabolites such as G-6-P and G-1-P, both of which are bound by PPAR α , albeit more weakly; (iii) additional proteins that also bind glucose (*e.g.* plasma membrane glucose transporters, hexokinase, nuclear proteins, etc.); (iv) competition of SRC-1 binding with other coactivators and corepressors; and (v) competition with other nuclear proteins that may compete with PPAR α for binding to DNA (*e.g.* HNF4 α in liver). Consequently, the cell lysate-based assays require considerably higher levels of glucose, and the changes elicited tend to be smaller. These issues are analogous to those observed for PPAR α -binding fatty acids and fatty acyl-CoAs with nM K_d values, whereas cell lysate-based assays (cofactor recruitment) required 100–1000-fold higher concentrations (3–5, 33).

Because glucose effects on transactivation of PPAR α and RXR α heterodimers were concentration-dependent, this suggests that PPAR α is not saturated at the lower end of physiological or dietary levels of glucose, even though the affinity of PPAR α for glucose is very high. Furthermore, this suggests that the free nuclear levels of glucose are low and less than the nuclear PPAR α levels. A parallel situation exists for PPAR α and fatty acid activation. Although PPAR α affinities for fatty acids and their metabolites (*i.e.* fatty acyl-CoAs) are in the low nanomolar range (3–5), transactivation assays and animal studies show that PPAR α is activated by physiological (μ M) and dietary (mM) levels of fatty acids (29–31, 39). Serum levels for fatty acids range from 0.3 to 1 mM depending on nutrient and/or diabetic status. However, free nuclear LCFA and LCFA-CoA concentrations are estimated to be in the range of 39–68 nM and 3 nM, respectively (17, 25). Such discrepancies between binding affinity and ligand concentration required for PPAR α transactivation and activation are most likely due to higher concentrations of PPAR α than free ligand within the nucleus.

Further, several studies suggest that glucose binding to PPAR α shown herein occurs at physiologically relevant glucose concentrations. Unlike most cells, liver cells express very high levels of PPAR α (300 μ M as estimated herein) and are freely permeable to glucose (40). Tissues other than liver are more insulin-responsive and have much lower intracellular glucose levels. For example, nuclear magnetic resonance imaging of muscle from normal and diabetic subjects showed that intracellular glucose concentrations were several orders of magnitude lower than in plasma (41). In muscle tissues, glucose and glucose metabolite levels are much closer to the respective affinities of PPAR α for these ligands. The effects of glucose on PPAR α binding to LCFA and LCFA-CoA were well within the range of nuclear LCFA and LCFA-CoA levels (17, 25). Liver homogenates contain 6 mM glucose, 11 μ M G-1-P, and 0.2 mM G-6-P total concentrations (15). These data suggest that depending on tissue type, the effects of both low and high glucose level may be physiologically significant.

Further, either nonspecific effects of high glucose or additional effects of glucose metabolites may also contribute lysate-based assays. With regards to the latter, for example, G-1-P shows effects at 11 μ M glucose. Thus, this glucose metabolite may be as physiologically relevant as glucose (or G-6-P) in interacting with PPAR α . It is possible that at low glucose levels, glucose itself is interacting with PPAR α , whereas at higher glu-

cose concentrations, the G-1-P or other metabolite may be interacting with PPAR α .

However, it is possible that in some cell types or tissues, free nuclear glucose concentrations are at a PPAR α saturating level. If in the future it is found that this is true, then this would indicate that the glucose-saturated PPAR α would be the physiological form for those cell types or tissues. Therefore, PPAR α assays would need to include saturating levels of glucose to be physiologically relevant with these cell types. Because glucose can enter liver cells through diffusion (40), liver may have elevated intracellular glucose levels, whereas other tissues may be glucose-deficient. In this case, perhaps altered nuclear glucose levels lead to the improper PPAR α activation found in diabetic patients (36, 42).

The data presented herein suggest a mechanistic role of PPAR α in the regulation of energy homeostasis by directly linking glucose and fatty acid oxidation. Previous work has shown that PPAR α is capable of binding fatty acyl-CoAs and unsaturated fatty acids with very high affinity (3–5). The data provide evidence that PPAR α also directly interacts with glucose and glucose metabolites with very high affinity, well within the range of normal physiological levels of these molecules in serum, cytoplasm, and nucleoplasm (15, 40, 41). This interaction altered PPAR α secondary structure and the ability of PPAR α to interact with lipidic ligands. Under basal conditions, glucose decreased PPAR α interaction with SRC-1 while increasing interaction with DNA. In the presence of activating ligands (fatty acids, fibrates), glucose increased PPAR α interaction with SRC-1, DNA binding, and activation of the β -oxidation pathway. These results suggest that hyperglycemic injury mediated by PPAR α occurs not only indirectly through elevated LCFA and LCFA-CoA levels but also as a direct action of glucose on PPAR α and through synergistic effects with xenobiotic and endogenous PPAR α activators.

Acknowledgments—We are very thankful to Noa Noy (Case Western Reserve University) for the PPAR α bacterial expression vector; Tso-Pang Yao (Duke University) for the SRC-1 mammalian expression vector; Sander Kersten (Wageningen University) for the PPAR α mammalian expression vector; Pierre Chambon (Université Louis Pasteur) for the RXR α mammalian expression vector; and Ronald Evans (Salk Institute) for the PPRE $_3$ -TK-LUC reporter construct. We also thank J. Bar-Tana and S. D. Rider for initial review of this manuscript.

REFERENCES

1. Zhang, Y., Lee, F. Y., Barrera, G., Lee, H., Vales, C., Gonzalez, F. J., Willson, T. M., and Edwards, P. A. (2006) *Proc. Natl. Acad. Sci. U. S. A.* **103**, 1006–1011
2. Kersten, S., Mandard, S., Escher, P., Gonzalez, F. J., Tafuri, S., Desvergne, B., and Wahli, W. (2001) *FASEB J.* **15**, 1971–1978
3. Lin, Q., Ruuska, S. E., Shaw, N. S., Dong, D., and Noy, N. (1999) *Biochemistry* **38**, 185–190
4. Hostetler, H. A., Petrescu, A. D., Kier, A. B., and Schroeder, F. (2005) *J. Biol. Chem.* **280**, 18667–18682
5. Hostetler, H. A., Kier, A. B., and Schroeder, F. (2006) *Biochemistry* **45**, 7669–7681
6. Corkey, B. E., Deeney, J. T., Yaney, G. C., and Tornheim, K. (2000) *J. Nutr.* **130**, 299S–304S
7. Mangelsdorf, D. J., and Evans, R. M. (1995) *Cell* **83**, 841–850
8. Desvergne, B., Michalik, L., and Wahli, W. (2004) *Mol. Endocrinology* **18**, 1321–1332

9. Frederiksen, K. S., Wulf, E. M., Wassermann, K., Sauerberg, P., and Fleckner, J. (2003) *J. Mol. Endocrinol.* **30**, 317–329
10. Kiec-Wilk, B., Dembinska-Kiec, A., Olszanecka, A., Bodzioch, M., and Kawecka-Jaszcz, K. (2005) *J. Phys. Pharm.* **56**, 149–162
11. Guerre-Millo, M., Rouault, C., Poulain, P., Andre, J., Poitout, V., Peters, J. M., Gonzalez, F. J., Fruchart, J.-C., Reach, G., and Staels, B. (2001) *Diabetes* **50**, 2809–2814
12. Forman, B. M., Tontonoz, P., Chen, J., Brun, R. P., Spiegelman, B. M., and Evans, R. M. (1995) *Cell* **83**, 803–812
13. Kliewer, S. A., Lenhard, J. M., Willson, T. M., Patel, I., Morris, D. C., and Lehmann, J. M. (1995) *Cell* **83**, 813–819
14. Hi, R., Osada, S., Yumoto, N., and Osumi, T. (1999) *J. Biol. Chem.* **274**, 35152–35158
15. Stewart, J. M., Dewling, V. F., and Wright, T. G. (1998) *Biochim. Biophys. Acta* **1391**, 1–6
16. Sreerama, N., and Woody, R. (2000) *Anal. Biochem.* **287**, 252–260
17. Huang, H., Starodub, O., McIntosh, A., Kier, A. B., and Schroeder, F. (2002) *J. Biol. Chem.* **277**, 29139–29151
18. Patsouris, D., Mandard, S., Voshol, P. J., Escher, P., Tan, N. S., Havekes, L. M., Koenig, W., Maerz, W., Tafuri, S., Wahli, W., Mueller, M., and Kersten, S. (2004) *J. Clin. Investig.* **114**, 94–103
19. Yao, T.-P., Ku, G., Zhou, N., Scully, R., and Livingston, D. M. (1996) *Proc. Natl. Acad. Sci. U. S. A.* **93**, 10626–10631
20. Leid, M., Kastner, P., Lyons, R., Nakshatri, H., Saunders, M., Zacharewski, T., Chen, J. Y., Staub, A., Garnier, J. M., Mader, S., and Chambon, P. (1992) *Cell* **58**, 377–395
21. Kliewer, S. A., Umesono, K., Noon, D. J., Heyman, R. A., and Evans, R. M. (1992) *Nature* **358**, 771–774
22. Spector, A. A., and Hoak, J. C. (1969) *Anal. Biochem.* **32**, 297–302
23. Keller, H., Dreyer, C., Medin, J., Mahfoudi, A., Ozato, K., and Wahli, W. (1993) *Proc. Natl. Acad. Sci. U. S. A.* **90**, 2160–2164
24. Gottlicher, M., Widmark, E., Li, Q., and Gustafsson, J. A. (1992) *Proc. Natl. Acad. Sci. U. S. A.* **89**, 4653–4657
25. Huang, H., Starodub, O., McIntosh, A., Atshaves, B. P., Woldegiorgis, G., Kier, A. B., and Schroeder, F. (2004) *Biochemistry* **43**, 2484–2500
26. Drochmans, P., Wanson, J.-C., and Mosselmans, R. (1975) *J. Cell Biol.* **66**, 1–22
27. Buira, I., Poch, E., Sanchez, O., Fernandez-Varo, G., Grau, M., Tebar, F., Ramirez, I., and Soley, M. (2004) *J. Cell Physiol.* **198**, 12–21
28. Wolfrum, C., Borrmann, C. M., Borchers, T., and Spener, F. (2001) *Proc. Natl. Acad. Sci. U. S. A.* **98**, 2323–2328
29. Wolfrum, C., Ellinghaus, P., Fobker, M., Seedorf, U., Assmann, G., Borchers, T., and Spener, F. (1999) *J. Lipid Res.* **40**, 708–714
30. Krey, G., Braissant, O., L'Horsset, F., Kalkhoven, E., Perroud, M., Parker, M. G., and Wahli, W. (1997) *Mol. Endocrinol.* **11**, 779–791
31. Banner, C. D., Gottlicher, M., Widmark, E., Sjoval, J., Rafter, J. J., and Gustafsson, J. (1993) *J. Lipid Res.* **34**, 1583–1591
32. Murakami, K., Ide, T., Nakazawa, T., Okazaki, T., Mochizuki, T., and Kadowaki, T. (2001) *Biochem. J.* **353**, 231–238
33. Elholm, M., Dam, I., Jorgensen, C., Krogsdam, A.-M., Holst, D., Kratchmarova, I., Gottlicher, M., Gustafsson, J. A., Berge, R. K., Flatmark, T., Knudsen, J., Mandrup, S., and Kristiansen, K. (2001) *J. Biol. Chem.* **276**, 21410–21416
34. Li, T., Lee, H. B., and Park, K. (1998) *J. Biomater. Sci. Polym. Ed.* **9**, 327–344
35. Cronet, P., Peterson, J. F. W., Folmer, R., Blomberg, N., Sjoblom, K., Karlsson, U., Lindstedt, E.-L., and Bamberg, K. (2001) *Structure* **9**, 699–706
36. Finck, B. N., Lehman, J. J., Leone, T. C., Welch, M. J., Bennett, M. J., Kovacs, A., Han, X., Gross, R. W., Kozak, R., Lopaschuk, G. D., and Kelly, D. P. (2002) *J. Clin. Investig.* **109**, 121–130
37. Fehr, M., Lalonde, S., Lager, I., Wolff, M. W., and Frommer, W. B. (2003) *J. Biol. Chem.* **278**, 1927–19133
38. Wasserman, D. H., and Halseth, A. E. (1998) *Adv. Exper. Med. Biol.* **441**, 1–16
39. Bonilla, S., Redonnet, A., Noel-Suberville, C., Pallet, V., Garcin, H., and Higuieret, P. (2000) *Br. J. Nutr.* **83**, 665–671
40. Voet, D., and Voet, J. G. (1990) *Biochemistry* (Voet, D., and Voet, J. G., eds) John Wiley & Sons, New York
41. Cline, G. W., Petersen, K. F., Krssak, M., Shen, J., Hundal, R. S., Trajanoski, Z., Inzucchi, S., Dresner, A., Rothman, D. L., and Shulman, G. I. (1999) *N. Engl. J. Med.* **341**, 240–246
42. Finck, B. N. (2004) *Curr. Op. Clin. Nutr. Metab. Care* **7**, 391–396

**Glucose Directly Links to Lipid Metabolism through High Affinity Interaction
with Peroxisome Proliferator-activated Receptor α**

Heather A. Hostetler, Huan Huang, Ann B. Kier and Friedhelm Schroeder

J. Biol. Chem. 2008, 283:2246-2254.

doi: 10.1074/jbc.M705138200 originally published online November 30, 2007

Access the most updated version of this article at doi: [10.1074/jbc.M705138200](https://doi.org/10.1074/jbc.M705138200)

Alerts:

- [When this article is cited](#)
- [When a correction for this article is posted](#)

[Click here](#) to choose from all of JBC's e-mail alerts

This article cites 41 references, 14 of which can be accessed free at
<http://www.jbc.org/content/283/4/2246.full.html#ref-list-1>